Inverse Problem in Refractive Index Based Optical Tomography

T. Khan* and A. Thomas
Department of Mathematical Sciences
Clemson University, Clemson, SC 29634-0975

ABSTRACT

In optical tomography, conventionally the diffusion approximation to the radiative transport equation (RTE) with a constant refractive index is used to image highly scattering or turbid media. Recently we derived the relevant RTE and its spherical harmonics or P_N approximation with a spatially varying refractive index. We found that the P_N model with spatially varying refractive index for photon transport is substantially different than the spatially constant model. In this report, we formulate the optical tomography inverse problem based on the diffusion or P_0 approximation to image a highly scattering medium with a spatially varying refractive index. We establish the theoretical framework for both the forward and the inverse problem for this formulation. We have simulated the forward and the inverse problem using the finite element method and have reconstructed the spatially varying refractive index parameter in our model for the inverse problem. Our simulations indicate that the refractive index based optical tomography shows promise for the reconstruction of the refractive index parameter.

Keywords: inverse problems, optical tomography, refractive index, highly scattering media, turbid media, Radiative transport, and biomedical imaging.

1 INTRODUCTION

In the last decade there has been considerable new development in bio-medical imaging using optical tomography [6, 1, 5, 19]. Optical tomography is a way to probe highly scattering media using low-energy visible or near infra-red light (NIR) and then to reconstruct images of these media. Light in the near-infrared range (wavelength from 700 to 1200 nm) penetrates tissue and interacts with it. The predominant effects are absorption and scattering [8, 11, 3]. The fundamental challenge in OT is that biological tissue is a highly scattering medium and the transport model deviates greatly from the Radon line integral model as in X-ray tomography. The widely accepted photon transport model is the radiative transfer equation (RTE). The

*Corresponding author (Email: khan@clemson.edu)

RTE is an integro-differential equation for the radiance and has spatially dependent diffusion and absorption parameters as coefficients which are a priori unknown. Hence the problem is to infer from the measurements of the photon density on the boundary, the coefficients of absorption and diffusion in the tissue. The solution to the RTE is not always tractable analytically or computationally, for example for a realistic tissue radius of 43 mm. Therefore a low order diffusion approximation to the RTE for a medium has been derived and studied in the context of optical imaging in the last several years. The diffusion approximation to the RTE has been widely used to calculate photon migration in biological tissues [12]. The existing computational methods for the inverse problem for photon migration in biological tissues are almost exclusively based on the diffusion approximation [4]. This is due to the simplicity of the diffusion approximation. However the associated optical tomography inverse problem using the diffusion approximation is exponentially ill-posed or unstable. This implies that image reconstruction is very sensitive to small errors in the data. This is why optical tomography is still not the choice for medical diagnostics similar to x-ray mammography.

Recent interest in the RTE for a medium with spatially varying refractive index is getting more attention [17, 18]. Media with spatially varying refractive index are among us in the form of biological tissues and the atmosphere, just to mention two examples [24, 23]. Recently we derived the relevant RTE and its spherical harmonics or P_N approximation for a highly scattering medium with a spatially varying refractive index. We found that the P_N model with spatially varying refractive index for photon transport is substantially different than the spatially constant model. In this report, we formulate the optical tomography inverse problem based on the diffusion or P_0 approximation for a highly scattering or turbid medium with a spatially varying refractive index. We establish the theoretical framework for both the forward and the inverse problem for this formulation. We simulate the forward and the inverse problem using the finite element method. We also derive the Fréchet derivative of the nonlinear inverse problem operator of refractive index based optical tomography.

The outline of the paper is as follows. In section 2, we derive the diffusion approximation for a medium with spatially varying refractive index. In section 3, we formulate the inverse problem. In section 4, we investigate the well-posedness of the forward model and the inverse problem. In section 5, we derive the Fréchet derivative. In section 6, we present our simulation results for inversion. In section 6, we discuss conclusions and future work.

2 RADIATIVE TRANSPORT FOR SPATIALLY VARYING REFRACTIVE INDEX

Let $\Omega \subset \mathbb{R}^d$ ($d = 2$ or $d = 3$) be simply connected, open, and bounded with boundary $\partial\Omega$ which is C^2. Then the radiative transfer equation with spatially refractive index is given by [17, 18]:

$$\begin{aligned} \frac{n}{c}\frac{\partial u}{\partial t}(\mathbf{x},\mathbf{s},t) &+ \mathbf{s}\cdot\nabla u(\mathbf{x},\mathbf{s},t) + \frac{1}{n}\nabla n\cdot\nabla_{\mathbf{s}} u(\mathbf{x},\mathbf{s},t) - \frac{2}{n}(\mathbf{s}\cdot\nabla n)u(\mathbf{x},\mathbf{s},t) \\ &+ (\mu_a+\mu_s)u(\mathbf{x},\mathbf{s},t) - \mu_s\int_{S^{d-1}}\Theta(\mathbf{s}\cdot\mathbf{s}')u(\mathbf{x},\mathbf{s}',t)d\mathbf{s} = f(\mathbf{x},\mathbf{s},t). \end{aligned}$$

where $\nu(\mathbf{x})$ denotes the outward unit normal, S^{d-1} is the unit sphere in R^d, $\mu_a(\mathbf{x})$ and $\mu_s(\mathbf{x})$ are the absorbtion and scattering coefficients respectively. We use the spherical harmonic expansion of u and f,

$$u(\mathbf{x},\mathbf{s},t) = \sum_{\ell=0}^{\infty}\sum_{m=-\ell}^{\ell}\left(\frac{2\ell+1}{4\pi}\right)^{1/2}\psi_{\ell,m}(\mathbf{x},t)Y_{\ell,m}(\mathbf{s}) \tag{1}$$

and

$$f(\mathbf{x},\mathbf{s},t) = \sum_{\ell=0}^{\infty}\sum_{m=-\ell}^{\ell}\left(\frac{2\ell+1}{4\pi}\right)^{1/2}f_{\ell,m}(\mathbf{x},t)Y_{\ell,m}(\mathbf{s}) \tag{2}$$

where $((2\ell+1)/4\pi)^{1/2}$ is the normalization factor. The phase function f can also be expressed using the addition theorem as,

$$\begin{aligned}\Theta(\mathbf{s}'\cdot\mathbf{s}) &= \sum_{\ell=0}^{\infty}\frac{2\ell+1}{4\pi}\Theta_\ell P_\ell(\mathbf{s}'\cdot\mathbf{s}) \\ &= \sum_{\ell=0}^{\infty}\sum_{m=-\ell}^{\ell}\Theta_\ell Y^*_{\ell,m}(\mathbf{s}')Y_{\ell,m}(\mathbf{s}).\end{aligned} \tag{3}$$

Substituting these expansions into (1) we get

$$\begin{aligned}\sum_{\ell=0}^{\infty}\sum_{m=-\ell}^{\ell} \quad & \left(\frac{2\ell+1}{4\pi}\right)^{1/2}\left[\left[\frac{n}{c}\frac{\partial}{\partial t}+\mathbf{s}\cdot\nabla\right.\right. \\ + \quad & \left.\frac{1}{n}\nabla n\cdot\nabla_{\mathbf{s}}-\frac{2}{n}(\mathbf{s}\cdot\nabla n)+\mu_t\right]\psi_{\ell,m}Y_{\ell,m}-f_{\ell,m}Y_{\ell,m} \\ - \quad & \left.\mu_s\int_{S^2}d\mathbf{s}'\psi_{\ell,m}Y_{\ell,m}(\mathbf{s}')\sum_{\ell'=0}^{\infty}\sum_{m'=-\ell'}^{\ell'}\Theta_{\ell'}Y^*_{\ell',m'}(\mathbf{s}')Y_{\ell',m'}(\mathbf{s})\right]=0\end{aligned} \tag{4}$$

where $\mu_t = \mu_s + \mu_a$ is the transport coefficient. The integral over $\mathbf{s}'$ can be calculated using the orthogonality relation for the spherical harmonics. Then equation (1) becomes

$$\begin{aligned}\sum_{\ell=0}^{\infty}\sum_{m=-\ell}^{\ell} \quad & \left(\frac{2\ell+1}{4\pi}\right)^{1/2}\left[\left[\frac{n}{c}\frac{\partial}{\partial t}+\mathbf{s}\cdot\nabla\right.\right. \\ + \quad & \left.\left.\frac{1}{n}\nabla n\cdot\nabla_{\mathbf{s}}-\frac{2}{n}(\mathbf{s}\cdot\nabla n)+\mu_t^n\right]\psi_{\ell,m}-f_{\ell,m}\right]Y_{\ell,m}=0\end{aligned} \tag{5}$$

where $\mu_t^\ell = \mu_s(1-\Theta_\ell)+\mu_a$ is the reduced transport coefficient. If we multiply equation (5) by $Y^*_{p,q}$ and integrate over $\mathbf{s}$ we can use the orthogonality relation in all terms except the terms with $\mathbf{s}\cdot\nabla$, $(\nabla n\cdot\nabla_{\mathbf{s}})/n$, and $-(2\mathbf{s}\cdot\nabla n)/n$. Therefore we arrive at

$$\left(\frac{2p+1}{4\pi}\right)^{1/2}\frac{n}{c}\frac{\partial}{\partial t}\psi_{p,q}+\left(\frac{2p+1}{4\pi}\right)^{1/2}\mu_t^p\psi_{p,q}$$

$$
\begin{aligned}
&+ \sum_{\ell=0}^{\infty}\sum_{m=-\ell}^{\ell}\int_{S^2}\left(\frac{2\ell+1}{4\pi}\right)^{1/2}\left[\mathbf{s}\cdot\nabla+\frac{1}{n}\nabla n\cdot\nabla_{\mathbf{s}}-\frac{2}{n}(\mathbf{s}\cdot\nabla n)\right]\psi_{\ell,m}Y_{\ell,m}Y^*_{p,q}d\mathbf{s}\\
&= \left(\frac{2p+1}{4\pi}\right)^{1/2} f_{p,q}. \qquad (6)
\end{aligned}
$$

Let

$$
\begin{aligned}
\alpha_p^q &:= \left(\frac{(p+q)(p+q+1)}{2p+1}\right)^{1/2}\\
\beta_p^q &:= \left(\frac{(p+q)(p+q-1)}{2p+1}\right)^{1/2}\\
\xi_p^q &:= \left(\frac{(p-q+1)(p+q+1)}{2p+1}\right)^{1/2}\\
\eta_p^q &:= \left(\frac{(p-q)(p+q)}{2p+1}\right)^{1/2}.
\end{aligned}
$$

Using these notations and analyzing the three terms involving the terms with $\mathbf{s}\cdot\nabla$, $(\nabla n\cdot\nabla_{\mathbf{s}})/n$, and $-(2\mathbf{s}\cdot\nabla n)/n$ and simplifying we get within the P_N approximation or the $N-$th order projection, see [18] for details, we find:

$$
\begin{aligned}
&(2p+1)^{1/2}\left(\frac{n}{c}\frac{\partial}{\partial t}+\mu_t^p\right)\psi_{p,q}+\eta_p^q\left[\frac{\partial}{\partial z}-\frac{2}{n}\frac{\partial n}{\partial z}\right]\psi_{p-1,q}\\
&+\beta_p^q\left[\frac{1}{n}\left(\frac{\partial n}{\partial x}-i\frac{\partial n}{\partial y}\right)-\frac{1}{2}\left(\frac{\partial}{\partial x}-i\frac{\partial}{\partial y}\right)\right]\psi_{p-1,q-1}\\
&-\beta_p^{-q}\left[\frac{1}{n}\left(\frac{\partial n}{\partial x}+i\frac{\partial n}{\partial y}\right)-\frac{1}{2}\left(\frac{\partial}{\partial x}+i\frac{\partial}{\partial y}\right)\right]\psi_{p-1,q+1}+\xi_p^q\left[\frac{\partial}{\partial z}-\frac{2}{n}\frac{\partial n}{\partial z}\right]\psi_{p+1,q}\\
&-\alpha_p^{-q+1}\left[\frac{1}{n}\left(\frac{\partial n}{\partial x}-i\frac{\partial n}{\partial y}\right)-\frac{1}{2}\left(\frac{\partial}{\partial x}-i\frac{\partial}{\partial y}\right)\right]\psi_{p+1,q-1}\\
&+\alpha_p^{q+1}\left[\frac{1}{n}\left(\frac{\partial n}{\partial x}+i\frac{\partial n}{\partial y}\right)-\frac{1}{2}\left(\frac{\partial}{\partial x}+i\frac{\partial}{\partial y}\right)\right]\psi_{p+1,q+1}\\
&+\sum_{\ell=0}^{N}\sum_{m=-\ell}^{\ell}\left(\frac{2\ell+1}{n^2}\right)^{1/2}\left[\frac{\partial n}{\partial x}\left[|m|I_1(\ell,m;p,q)+\rho(\ell,m)I_2(\ell,m;p,q)\right.\right.\\
&-(im)I_3(\ell,m;p,q)]+\frac{\partial n}{\partial y}\left[|m|I_4(\ell,m;p,q)+\rho(\ell,m)I_5(\ell,m;p,q)\right.\\
&\left.\left.+(im)I_6(\ell,m;p,q)]-\frac{\partial n}{\partial z}\left[|m|I_7(\ell,m;p,q)+\rho(\ell,m)I_8(\ell,m;p,q)\right]\right]\psi_{\ell,m}\\
&=(2p+1)^{1/2}f_{p,q} \qquad (7)
\end{aligned}
$$

where,

$$
I_1(\ell,m) := \int_0^{2\pi}\int_0^{\pi}(\cos^2\vartheta\cos\varphi)Y_{\ell,m}Y^*_{p,q}d\vartheta d\varphi
$$

$$
\begin{aligned}
I_2(\ell,m) &:= \int_0^{2\pi}\int_0^{\pi}(\cos\vartheta\cos\varphi\sin\vartheta)e^{-i\sigma_m\varphi}Y_{\ell,m+\sigma_m}Y^*_{p,q}d\vartheta d\varphi \\
I_3(\ell,m) &:= \int_0^{2\pi}\int_0^{\pi}\sin\varphi Y_{\ell,m}Y^*_{p,q}d\vartheta d\varphi \\
I_4(n,m) &:= \int_0^{2\pi}\int_0^{\pi}(\cos^2\vartheta\sin\varphi)Y_{\ell,m}Y^*_{p,q}d\vartheta d\varphi \\
I_5(\ell,m) &:= \int_0^{2\pi}\int_0^{\pi}(\cos\vartheta\sin\varphi\sin\vartheta)e^{-i\sigma_m\varphi}Y_{\ell,m+\sigma_m}Y^*_{p,q}d\vartheta d\varphi \\
I_6(\ell,m) &:= \int_0^{2\pi}\int_0^{\pi}\cos\varphi Y_{\ell,m}Y^*_{p,q}d\vartheta d\varphi \\
I_7(\ell,m) &:= \int_0^{2\pi}\int_0^{\pi}(\cot\vartheta\sin^2\vartheta)Y_{\ell,m}Y^*_{p,q}d\vartheta d\varphi \\
I_8(\ell,m) &:= \int_0^{2\pi}\int_0^{\pi}(\sin^2\vartheta)e^{-i\sigma_m\varphi}Y_{\ell,m+\sigma_m}Y^*_{p,q}d\vartheta d\varphi.
\end{aligned}
$$

The above integrals I_1 through I_8 are computed in [18] along with the details of the derivation of the P_N approximation.

2.1 P_1 Approximation

The P_1 approximation is obtained by assuming that $\psi_{\ell,m}=0$ for $\ell>1$. In this case we get four equations which we will find the general form of using (7) by letting $N=1$:

$$
\begin{aligned}
&(2p+1)^{1/2}\left(\frac{n}{c}\frac{\partial}{\partial t}+\mu_t^p\right)\psi_{p,q}+\eta_p^q\left[\frac{\partial}{\partial z}-\frac{2}{n}\frac{\partial n}{\partial z}\right]\psi_{p-1,q} \\
&+\beta_p^q\left[\frac{1}{n}\left(\frac{\partial n}{\partial x}-i\frac{\partial n}{\partial y}\right)-\frac{1}{2}\left(\frac{\partial}{\partial x}-i\frac{\partial}{\partial y}\right)\right]\psi_{p-1,q-1} \\
&-\beta_p^{-q}\left[\frac{1}{n}\left(\frac{\partial n}{\partial x}+i\frac{\partial n}{\partial y}\right)-\frac{1}{2}\left(\frac{\partial}{\partial x}+i\frac{\partial}{\partial y}\right)\right]\psi_{p-1,q+1}+\xi_p^q\left[\frac{\partial}{\partial z}-\frac{2}{n}\frac{\partial n}{\partial z}\right]\psi_{p+1,q} \\
&-\alpha_p^{-q+1}\left[\frac{1}{n}\left(\frac{\partial n}{\partial x}-i\frac{\partial n}{\partial y}\right)-\frac{1}{2}\left(\frac{\partial}{\partial x}-i\frac{\partial}{\partial y}\right)\right]\psi_{p+1,q-1} \\
&+\alpha_p^{q+1}\left[\frac{1}{n}\left(\frac{\partial n}{\partial x}+i\frac{\partial n}{\partial y}\right)-\frac{1}{2}\left(\frac{\partial}{\partial x}+i\frac{\partial}{\partial y}\right)\right]\psi_{p+1,q+1} \\
&+\sum_{\ell=0}^{1}\sum_{m=-\ell}^{\ell}\left(\frac{2\ell+1}{n^2}\right)^{1/2}\left[\frac{\partial n}{\partial x}\left[|m|I_1(\ell,m;p,q)+\rho(\ell,m)I_2(\ell,m;p,q)\right.\right. \\
&-(im)I_3(\ell,m;p,q)]+\frac{\partial n}{\partial y}\left[|m|I_4(\ell,m;p,q)+\rho(\ell,m)I_5(\ell,m;p,q)\right. \\
&\left.\left.+(im)I_6(\ell,m;p,q)]-\frac{\partial n}{\partial z}\left[|m|I_7(\ell,m;p,q)+\rho(\ell,m)I_8(\ell,m;p,q)\right]\right]\psi_{\ell,m} \\
&=(2p+1)^{1/2}f_{p,q}
\end{aligned}
\tag{8}
$$

We will use (8) to find the four equations with some simplification we get The P_1 approximation is given by the following four equations:

$$\left(\frac{n}{c}\frac{\partial}{\partial t}+\mu_t^0\right)\psi_{0,0}+\frac{\partial}{\partial z}\psi_{1,0}+\frac{1}{\sqrt{2}}\left(\frac{\partial}{\partial x}-i\frac{\partial}{\partial y}\right)\psi_{1,-1}-\frac{1}{\sqrt{2}}\left(\frac{\partial}{\partial x}+i\frac{\partial}{\partial y}\right)\psi_{1,1}=f_{0,0} \tag{9}$$

$$\left(\frac{n}{c}\frac{\partial}{\partial t}+\mu_t^1\right)\psi_{1,-1}-\frac{\sqrt{2}}{3}\left[\frac{1}{n}\left(\frac{\partial n}{\partial x}+i\frac{\partial n}{\partial y}\right)-\frac{1}{2}\left(\frac{\partial}{\partial x}+i\frac{\partial}{\partial y}\right)\right]\psi_{0,0}=f_{1,-1} \tag{10}$$

$$\left(\frac{n}{c}\frac{\partial}{\partial t}+\mu_t^1\right)\psi_{1,0}+\frac{1}{3}\left(\frac{\partial}{\partial z}-\frac{2}{n}\frac{\partial n}{\partial z}\right)\psi_{0,0}=f_{1,0} \tag{11}$$

$$\left(\frac{n}{c}\frac{\partial}{\partial t}+\mu_t^1\right)\psi_{1,1}+\frac{\sqrt{2}}{3}\left[\frac{1}{n}\left(\frac{\partial n}{\partial x}-i\frac{\partial n}{\partial y}\right)-\frac{1}{2}\left(\frac{\partial}{\partial x}-i\frac{\partial}{\partial y}\right)\right]\psi_{0,0}=f_{1,1} \tag{12}$$

.

When the refractive index n is taken to be the constant 1, then (9)-(12) reduce to

$$\left(\frac{1}{c}\frac{\partial}{\partial t}+\mu_t^0\right)\psi_{0,0}+\left(\frac{\partial}{\partial z}\right)\psi_{1,0}+\frac{1}{\sqrt{2}}\left(\frac{\partial}{\partial x}-i\frac{\partial}{\partial y}\right)\psi_{1,-1}-\frac{1}{\sqrt{2}}\left(\frac{\partial}{\partial x}+i\frac{\partial}{\partial y}\right)\psi_{1,1}=f_{0,0}$$

$$\left(\frac{1}{c}\frac{\partial}{\partial t}+\mu_t^1\right)\psi_{1,-1}+\frac{\sqrt{2}}{6}\left(\frac{\partial}{\partial x}+i\frac{\partial}{\partial y}\right)\psi_{0,0}=f_{1,-1}$$

$$\left(\frac{1}{c}\frac{\partial}{\partial t}+\mu_t^1\right)\psi_{1,0}+\frac{1}{3}\left(\frac{\partial}{\partial z}\right)\psi_{0,0}=f_{1,0}$$

$$\left(\frac{1}{c}\frac{\partial}{\partial t}+\mu_t^1\right)\psi_{1,1}-\frac{\sqrt{2}}{6}\left(\frac{\partial}{\partial x}-i\frac{\partial}{\partial y}\right)\psi_{0,0}=f_{1,1}$$

which is consistent with Arridge [1].

2.2 P_0 or Diffusion Approximation

Let

$$\mathbf{u}_1(\mathbf{x},t) = \frac{1}{4\pi}\int_{S^2}\mathbf{s}u(\mathbf{x},\mathbf{s},t)d\mathbf{s} = \frac{1}{4\pi}\begin{pmatrix}\frac{1}{\sqrt{2}}[\psi_{1,-1}(\mathbf{x},t)-\psi_{1,1}(\mathbf{x},t)]\\ \frac{1}{i\sqrt{2}}[\psi_{1,-1}(\mathbf{x},t)+\psi_{1,1}(\mathbf{x},t)]\\ \psi_{1,0}(\mathbf{x},t)\end{pmatrix} \tag{13}$$

$$u(\mathbf{x},t) = \frac{1}{4\pi}\int_{S^2}u(\mathbf{x},\mathbf{s},t)d\mathbf{s} = \frac{1}{4\pi}\psi_{0,0}(\mathbf{x},t). \tag{14}$$

We define f_0 and $\mathbf{f}_1$ by

$$f_0(\mathbf{x},t) = \frac{1}{4\pi}f_{0,0}(\mathbf{x},t) \tag{15}$$

$$\mathbf{f}_1(\mathbf{x},t) = \frac{1}{4\pi}\int_{S^2}\mathbf{s}f(\mathbf{x},\mathbf{s},t)d\mathbf{s} = \begin{pmatrix}\frac{1}{\sqrt{2}}[f_{1,-1}(\mathbf{x},t)-f_{1,1}(\mathbf{x},t)]\\ \frac{1}{i\sqrt{2}}[f_{1,-1}(\mathbf{x},t)+f_{1,1}(\mathbf{x},t)]\\ f_{1,0}(\mathbf{x},t)\end{pmatrix}. \tag{16}$$

Using (13)-(16) we may write the P_1 approximation in the form

$$\left(\frac{n}{c}\frac{\partial}{\partial t} + \mu_t^0\right) u(\mathbf{x},t) + \nabla \cdot \mathbf{u}_1(\mathbf{x},t) = f_0(\mathbf{x},t) \tag{17}$$

$$\left(\frac{n}{c}\frac{\partial}{\partial t} + \mu_t^1\right) \mathbf{u}_1(\mathbf{x},t) + \frac{1}{3}\left(\nabla - \frac{2}{n}\nabla n\right) u(\mathbf{x},t) = \mathbf{f}_1(\mathbf{x},t). \tag{18}$$

The diffusion or P_0 approximation is obtained by assuming that

$$\frac{\partial \mathbf{u}_1}{\partial t}(\mathbf{x},t) = 0 \qquad \text{and} \qquad \mathbf{f}_1(\mathbf{x},t) = 0.$$

We refer to Arridge [1], Khan et al. [15, 14], Marti-Lopez et al. [21, 20] for a detailed discussion about the assumptions and the validity of the diffusion approximation. Under these assumptions, (18) becomes

$$\mu_t^1 \mathbf{u}_1(\mathbf{x},t) + \frac{1}{3}\left(\nabla - \frac{2}{n}\nabla n\right) u(\mathbf{x},t) = 0.$$

Solving for $\mathbf{u}_1(\mathbf{x},t)$ we arrive at

$$\begin{aligned} \mathbf{u}_1(\mathbf{x},t) &= \frac{-1}{3\mu_t^1}\left(\nabla - \frac{2}{n}\nabla n\right) u(\mathbf{x},t) \\ &= -D(\mathbf{x})\left(\nabla - \frac{2}{n}\nabla n\right) u(\mathbf{x},t) \end{aligned}$$

where $D = 1/(3\mu_t^1)$ is the diffusion coefficient. Substituting this into (17) yields

$$\left(\frac{n}{c}\frac{\partial}{\partial t} + \mu_t^0\right) u(\mathbf{x},t) - \nabla \cdot \left[D(\mathbf{x})\left(\nabla - \frac{2}{n}\nabla n\right) u(\mathbf{x},t)\right] = f_0(\mathbf{x},t). \tag{19}$$

The frequency domain refractive index diffusion approximation can be obtained by Fourier transformation of the equation (19):

$$\left(\frac{i\omega n}{c} + \mu_a\right) u(\mathbf{x},\omega) - \nabla \cdot \left[D(\mathbf{x})\left(\nabla - \frac{2}{n}\nabla n\right) u(\mathbf{x},\omega)\right] = f_0(\mathbf{x},\omega).$$

For DC optical tomography, it is sufficient to use the time independent simplification of this equation [1, 13]:

$$\mu_a u(\mathbf{x}) - \nabla \cdot \left[D(\mathbf{x})\left(\nabla - \frac{2}{n}\nabla n\right) u(\mathbf{x})\right] = f_0(\mathbf{x}). \tag{20}$$

2.3 Boundary Condition

The flux over the boundary is modelled by the condition

$$u(\mathbf{x},\mathbf{s},t) = g^-(\mathbf{x},\mathbf{s},t) \quad \text{for} \quad \mathbf{x} \in \partial\Omega, \quad \nu(\mathbf{x}) \cdot \mathbf{s} \leq 0, \quad t \geq 0$$

where ν is the outwardly oriented normal vector on $\partial\Omega$. From this we obtain

$$\nu(\mathbf{x}) \cdot \int_{\nu(\mathbf{x})\cdot\mathbf{s}\leq 0} \mathbf{s}u(\mathbf{x},\mathbf{s},t)d\mathbf{s} = \nu(\mathbf{x}) \cdot \int_{\nu(\mathbf{x})\cdot\mathbf{s}\leq 0} \mathbf{s}g^{-}(\mathbf{x},\mathbf{s},t)d\mathbf{s} \tag{21}$$

for $\mathbf{x} \in \partial\Omega$, $t \geq 0$. We have from [17, 18] that $\mathbf{u}_1$ may be approximated by

$$\mathbf{u}_1(\mathbf{x},t) = -D\left(\nabla - \frac{2}{n}\nabla n\right) u(\mathbf{x},t) \tag{22}$$

analogous with Fick's law. If we further assume that u depends only linearly on $\mathbf{s}$, i.e.

$$u(\mathbf{x},\mathbf{s},t) \;\; = \;\; c_0 u_0(\mathbf{x},t) + c_1 \mathbf{s}\cdot\mathbf{u}_1(\mathbf{x},t)$$

and using (22), we get that

$$u(\mathbf{x},\mathbf{s},t) = u(\mathbf{x},t) - 3\mathbf{s}\cdot D\left(\nabla - \frac{2}{n}\nabla n\right) u(\mathbf{x},t). \tag{23}$$

Using the substitution (23), we may evaluate (21) for an isotropic distribution $g^{-}(\mathbf{x},\mathbf{s},t) = g^{-}(\mathbf{x},t)$ under the observation that

$$\nu \cdot \int_{\nu\cdot\mathbf{s}\leq 0} \mathbf{s}d\mathbf{s} = -\pi, \quad \text{and} \quad \nu \cdot \int_{\nu\cdot\mathbf{s}\leq 0} \mathbf{s}_i\mathbf{s}_j d\mathbf{s} = \begin{cases} 0 & i \neq j \\ \frac{2\pi}{3}\nu_i & i = j \end{cases}$$

thus arriving at

$$-\pi u(\mathbf{x},t) - 2\pi D\nu(\mathbf{x})\cdot\left(\nabla - \frac{2}{n}\nabla n\right) u(\mathbf{x},t) = -\pi g^{-}(\mathbf{x},t)$$

This may be written simply as

$$u + 2D\left(\frac{\partial}{\partial\nu} - \frac{2}{n}\frac{\partial n}{\partial\nu}\right) u = g^{-} \tag{24}$$

and is the boundary condition for our diffusion model.

2.4 Equation for Measurements

The measurements taken are

$$g(\mathbf{x},t) = \frac{1}{4\pi}\int_{S^2} \nu(\mathbf{x})\cdot\mathbf{s}u(\mathbf{x},\mathbf{s},t)d\mathbf{s}, \quad \mathbf{x}\in\partial\Omega, \quad t\geq 0$$

which may be approximated using (22) as

$$g(\mathbf{x},t) = \nu(\mathbf{x})\cdot\mathbf{u}_1(\mathbf{x},t) = -D\nu(\mathbf{x})\cdot\left(\nabla - \frac{2}{n}\nabla n\right) u(\mathbf{x},t)$$

or simply

$$g = -D\left(\frac{\partial}{\partial\nu} - \frac{2}{n}\frac{\partial n}{\partial\nu}\right) u \quad \text{on} \quad \partial\Omega$$

3 FORMULATION OF THE REFRACTIVE INDEX INVERSE PROBLEM

Now, we can define the forward problem as: given sources f_j in Ω and $\mathbf{q}$ in Q, a vector of model parameters, for example the coefficient of diffusion D, spatially varying refractive index n, and the coefficient of absorption μ_a (i.e. $\mathbf{q} = (D, n, \mu_a)^T$) that belongs to a parameter set Q, find the data u on $\partial\Omega$ and the inverse problem as: given data z on $\partial\Omega$ find $\mathbf{q}$. We can recast the forward problem in an abstract setting as the following parameter dependent equation:

$$\left(\frac{n}{c}\frac{\partial}{\partial t} + \mu_t^0\right) u(\mathbf{x}, t; \mathbf{q}) - \nabla \cdot \left[D(\mathbf{x})\left(\nabla - \frac{2}{n}\nabla n\right) u(\mathbf{x}, t; \mathbf{q})\right] = f_0(\mathbf{x}, t; \mathbf{q}). \tag{25}$$

where $\mathbf{x}$ is in Ω, $u(\mathbf{q})$ is in an appropriate abstract space H, and f represents a source or a forcing distribution. In general, measurement of $u(\mathbf{q})$ may not be possible, only some observable part $\mathcal{C}u(\mathbf{q})$ of the actual state $u(\mathbf{q})$ may be measured. In this abstract setting, the objective of the inverse or parameter estimation problem is to choose a parameter $\mathbf{q}^*$ in Q, that minimizes an error criterion or cost functional $J(u(\mathbf{q}), \mathcal{C}u(\mathbf{q}), \mathbf{q})$ over all possible $\mathbf{q}$ in Q subject to $u(\mathbf{q})$ satisfying the diffusion approximation. A typical observation operator is,

$$\mathcal{C}^f u(\mathbf{q}) \;=\; \left\{-D\frac{\partial u}{\partial \nu}(\mathbf{x}_i; \mathbf{q}, f)\right\}_{i=1}^{m} \tag{26}$$

where $\mathbf{x}_i$ is in $\partial\Omega$, m is the number of measurements. A typical cost functional $\mathbf{J}_\lambda$ is given as,

$$J_\lambda(\mathbf{q}) \;=\; \frac{1}{2}\sum_{j=1}^{m_s}\sum_{i=1}^{m}\left|\mathcal{C}_i^{f_j} u(\mathbf{q}) - z_i^{f_j}\right|^2 + \lambda\|\mathbf{q} - \mathbf{q}_0\|^2 \tag{27}$$

where $z_i^{f_j}$ is the measured data at the boundary for a given source f_j and λ is the Tikhonov regularization parameter. Now composing $u(\mathbf{q})$ and $\mathcal{C}u(\mathbf{q})$ we obtain the parameter-to-output mapping: $T[\mathbf{q}] = \mathcal{C}u$. This is the nonlinear mapping of refractive index based diffusion optical tomography in abstract setting.

4 WELL-POSEDNESS OF THE FORWARD PROBLEM

We shall now devote our attention to the weak formulation of the boundary value problem

$$\begin{aligned} \mu_a u(\mathbf{x}) - \nabla \cdot \left[D(\mathbf{x})\left(\nabla - \frac{2}{n}\nabla n\right) u(\mathbf{x})\right] &= f_0(\mathbf{x}) \quad \text{in} \quad \Omega \\ u(\mathbf{x}) + 2D(\mathbf{x})\left(\frac{\partial}{\partial \nu} - \frac{2}{n}\frac{\partial n}{\partial \nu}\right) u(\mathbf{x}) &= g^-(\mathbf{x}) \quad \text{on} \quad \partial\Omega. \end{aligned} \tag{28}$$

We begin by introducing a Hilbert space we shall denote by $V(\Omega)$ and in which we will do our analysis. The reader should note that this space was first introduced by Maz'ja [22] and has been applied by Daners [7] to Robin BVP's defined on general domains. Define the inner product $\langle \cdot, \cdot \rangle_V$ by

$$\langle u, v \rangle_V := \langle \nabla u, \nabla v \rangle_{L^2(\Omega)} + \langle u|_{\partial\Omega}, v|_{\partial\Omega} \rangle_{L^2(\partial\Omega)} \tag{29}$$

then $\| \cdot \|_V$, given by

$$\|u\|_V := \left(\|\nabla u\|^2_{L^2(\Omega)} + \|u|_{\partial\Omega}\|^2_{L^2(\partial\Omega)} \right)^{\frac{1}{2}}, \tag{30}$$

is the norm induced by this inner product. We define the space $V(\Omega)$ to be the closure of

$$\left\{ u \in W^1_2(\Omega) \cap \mathcal{C}(\bar{\Omega}) \cap \mathcal{C}^\infty(\Omega) : \|u\|_V < \infty \right\}$$

with respect to $\| \cdot \|_V$. We claim that $V(\Omega)$ is equal to $H^1(\Omega)$ up to equivalent norm. Appropriate smoothness conditions on $\partial\Omega$ allow us to gather from the Sobolev Trace Theorem for Lipschitz domains (see [9]) that $\|u|_{\partial\Omega}\|_{L^2(\partial\Omega)} \leq (c-1)\|u\|_{H^1(\Omega)}$ for some $c > 1$. Thus

$$\|u\|^2_V = \|\nabla u\|^2_{L^2(\Omega)} + \|u|_{\partial\Omega}\|^2_{L^2(\partial\Omega)} \leq c\|u\|^2_{H^1(\Omega)}.$$

The weak form of (28) is obtained by multiplying both sides of (20) by a function $v(\mathbf{x})$ and integrating over the spatial domain Ω:

$$\int_\Omega \mu_a u v d\mathbf{x} - \int_\Omega \nabla \cdot \left[D \left(\nabla - \frac{2}{n} \nabla n \right) u \right] v d\mathbf{x} = \int_\Omega f_0 v d\mathbf{x}$$

Integrating by parts and applying the boundary condition (24) yields

$$\int_\Omega D \left(\nabla - \frac{2}{n} \nabla n \right) u \cdot \nabla v d\mathbf{x} + \int_\Omega \mu_a u v d\mathbf{x} + \frac{1}{2} \int_{\partial\Omega} (u - g^-) v ds = \int_\Omega f_0 v d\mathbf{x}$$

We let F be a second primitive of f_0 so that $f_0 = \nabla \cdot \nabla F$, thus arriving at

$$\begin{aligned} \int_\Omega D \left(\nabla - \frac{2}{n} \nabla n \right) u \cdot \nabla v d\mathbf{x} \;&+\; \int_\Omega \mu_a u v d\mathbf{x} + \frac{1}{2} \int_{\partial\Omega} u v ds \\ &= \int_\Omega (\nabla \cdot \nabla F) v d\mathbf{x} + \frac{1}{2} \int_{\partial\Omega} g^- v ds. \end{aligned}$$

Under the assumption that the support of f_0 is properly contained in the interior of Ω, we integrate by parts again to obtain the weak form

$$\begin{aligned} \int_\Omega D \left(\nabla - \frac{2}{n} \nabla n \right) u \cdot \nabla v d\mathbf{x} \;&+\; \int_\Omega \mu_a u v d\mathbf{x} + \frac{1}{2} \int_{\partial\Omega} u v ds \\ &= -\int_\Omega \nabla F \cdot \nabla v d\mathbf{x} + \frac{1}{2} \int_{\partial\Omega} g^- v ds \end{aligned} \tag{31}$$

Define the bilinear form $B[\cdot,\cdot]$ by

$$B[u,v] = \int_\Omega D\nabla u\cdot\nabla v d\mathbf{x} \;-\; \int_\Omega D\frac{2}{n}\nabla n u\cdot\nabla v d\mathbf{x} + \int_\Omega \mu_a uv d\mathbf{x} + \frac{1}{2}\int_{\partial\Omega} uv ds \tag{32}$$

Then we may express (31) as

$$B[u,v] = \langle G, v\rangle_V \quad \text{for all} \quad v\in V(\Omega) \tag{33}$$

where

$$G(\mathbf{x}) := \begin{cases} -F(\mathbf{x}) & \text{in} \quad \Omega \\ \frac{1}{2}g^-(\mathbf{x}) & \text{on} \quad \partial\Omega. \end{cases}$$

We will proceed to verify the continuity and coercivity conditions of the Lax-Milgram Theorem for the form $B[\cdot,\cdot]$, thus showing that (31) has a unique solution $u\in V$ for all $v\in V$.

4.1 Continuity

Suppose that $0<b_1<D(\mathbf{x})$, $\|D\|_\infty\le a_1$, $\|\mu_a\|_\infty\le a_2$, and that $\|\frac{2}{n}\nabla n\|_\infty\le a_3$. Also let a_4 satisfy $\|v\|_{L^2(\Omega)}\le a_4\|v\|_V$ for all $v\in V$. Then

$$|B[u,v]| \le a_1\int_\Omega |\nabla u\cdot\nabla v| d\mathbf{x} + a_1a_3\int_\Omega |u\cdot\nabla v| d\mathbf{x} + a_2\int_\Omega |uv| d\mathbf{x} + \frac{1}{2}\int_{\partial\Omega}|uv| ds.$$

Applying Hölder's Inequality we get

$$\begin{aligned} |B[u,v]| \le\; & a_1\left(\int_\Omega |\nabla u|^2 d\mathbf{x}\right)^{1/2}\left(\int_\Omega |\nabla v|^2 d\mathbf{x}\right)^{1/2} \\ & + a_1a_3\left(\int_\Omega |u|^2 d\mathbf{x}\right)^{1/2}\left(\int_\Omega |\nabla v|^2 d\mathbf{x}\right)^{1/2} \\ & + a_2\left(\int_\Omega |u|^2 d\mathbf{x}\right)^{1/2}\left(\int_\Omega |v|^2 d\mathbf{x}\right)^{1/2} \\ & + \frac{1}{2}\left(\int_{\partial\Omega} |u|^2 ds\right)^{1/2}\left(\int_{\partial\Omega} |v|^2 ds\right)^{1/2} \\ \le\; & a_1\left(\|\nabla u\|^2_{L^2(\Omega)} + \|u|_{\partial\Omega}\|^2_{L^2(\partial\Omega)}\right)^{1/2}\left(\|\nabla v\|^2_{L^2(\Omega)} + \|v|_{\partial\Omega}\|^2_{L^2(\partial\Omega)}\right)^{1/2} \\ & + a_1a_3\|u\|_{L^2(\Omega)}\left(\|\nabla v\|^2_{L^2(\Omega)} + \|v|_{\partial\Omega}\|^2_{L^2(\partial\Omega)}\right)^{1/2} \\ & + a_2\|u\|_{L^2(\Omega)}\|v\|_{L^2(\Omega)} \end{aligned}$$

$$
\begin{aligned}
&+\frac{1}{2}\left(\|\nabla u\|^2_{L^2(\Omega)}+\|u|_{\partial\Omega}\|^2_{L^2(\partial\Omega)}\right)^{1/2}\left(\|\nabla v\|^2_{L^2(\Omega)}+\|v|_{\partial\Omega}\|^2_{L^2(\partial\Omega)}\right)^{1/2}\\
\leq\quad &\left(a_1+a_1a_3a_4+a_2a_4^2+\frac{1}{2}\right)\|u\|_V\|v\|_V.
\end{aligned}
$$

Letting $\alpha=\left(a_1+a_1a_3a_4+a_2a_4^2+\frac{1}{2}\right)$ we obtain $|B[u,v]|\leq\alpha\|u\|_V\|v\|_V$ as desired.

4.2 Coercivity

Now consider

$$
\begin{aligned}
|B[u,u]| &\geq \int_\Omega D|\nabla u|^2d\mathbf{x}-\int_\Omega D\frac{2}{n}\nabla nu\cdot\nabla ud\mathbf{x}+\int_\Omega\mu_a|u|^2d\mathbf{x}+\frac{1}{2}\int_{\partial\Omega}|u|^2ds\\
&\geq \min\left\{b_1,\frac{1}{2}\right\}\|u\|^2_V-\int_\Omega D\frac{2}{n}\nabla nu\cdot\nabla ud\mathbf{x}+\int_\Omega\mu_a|u|^2d\mathbf{x}.
\end{aligned}
$$

Taking note that $\mu_a(\mathbf{x})\geq 0$ for all $\mathbf{x}\in\Omega$ we may neglect the last integral and write

$$
|B[u,u]| \geq \min\left\{b_1,\frac{1}{2}\right\}\|u\|^2_V-\int_\Omega D\frac{2}{n}\nabla nu\cdot\nabla ud\mathbf{x}.
$$

Using Hölder's Inequality to estimate the second integral, we get:

$$
\begin{aligned}
|B[u,u]| &\geq \min\left\{b_1,\frac{1}{2}\right\}\|u\|^2_V-a_1a_3\left(\int_\Omega|u|^2d\mathbf{x}\right)^{1/2}\left(\int_\Omega|\nabla u|^2d\mathbf{x}\right)^{1/2}\\
&\geq \min\left\{b_1,\frac{1}{2}\right\}\|u\|^2_V-a_1a_3a_4\|u\|^2_V.
\end{aligned}
$$

Letting $\beta=\min\{b_1,1/2\}-a_1a_3a_4$ and if we assume further that $\beta>0$, we obtain $\beta\|u\|^2_{H^1}\leq|B[u,u]|$.

Having satisfied the continuity and coercivity conditions of the Lax-Milgram Lemma (see [10]), we conclude that the boundary value problem (28) has a unique solution u which satisfies the a priori esimate

$$
\|u\|_V\leq C\|G\|_V \tag{34}
$$

for some constant $C>0$ which is dependent only on the parameters D,μ_a and n. Otherwise stated, (34) may be written as

$$
\|u\|^2_{L^2(\Omega)}+\|u|_{\partial\Omega}\|^2_{L^2(\partial\Omega)}\leq C^2\left(\|F\|^2_{L^2(\Omega)}+\|g^-\|^2_{L^2(\partial\Omega)}\right) \tag{35}
$$

which implies the solution is continuous with respect to data.

5 WELL-POSEDNESS OF THE INVERSE PROBLEM

In this section, for convenience we will redefine $\mathbf{q}$ as

$$
\mathbf{q}=(D,\mathbf{n}_g,\mu_a)
$$

where $\mathbf{n}_g = \nabla \ln(n)$. We note that the definition makes sense physically as refractive index n is always greater than or equal to one. Let $Q = W^{1,p}(\Omega) \times \otimes_{i=1}^{d} L^\infty(\Omega) \times L^\infty(\Omega)$ where $W^{k,p}$ is the standard Sobolev space with the norm $\|\cdot\|_{W^{k,p}}$ and $p > 1$. Suppose Q_1 is the subspace of Q such that

$$Q_1 = \{\mathbf{q} \in Q : \|D\|_{W^{1,p}} \leq \alpha_1, \|\mathbf{n}_g\|_{L^\infty} \leq \alpha_2, \|\mu_a\|_{L^\infty} \leq \alpha_3\}. \tag{36}$$

Now Q_1 endowed with the topology

$$W^{1,p}_{weak} \times \otimes_{i=1}^{d} L^\infty_{weak^*} \times L^\infty_{weak^*} \tag{37}$$

is a metric space. This follows from the facts i) $W^{1,p}_{weak}$ is metrizable because closed unit sphere of a reflexive Banach space is compact in weak topology and ii) the $L^\infty_{weak^*}$ coordinates are metrizable because these coordinates can be shown to be compact using Aloglu's theorem together with separability of L^1. If we further restrict our parameter set Q_1 to the following

$$\tilde{Q} = \{\mathbf{q} \in Q_1 : \|D\|_{W^{1,p}} \leq \alpha_1, \|\mathbf{n}_g\|_{L^\infty} \leq \alpha_2, \bar{\mu} < \|\mu_a\|_{L^\infty} \leq \alpha_3\}. \tag{38}$$

It can be shown that $\tilde{Q}$ is a compact subset of Q, we refer the reader to Lemma 1.3 p. 223 [2] for further details. It can also be shown that there exists unique weak solution $u(\mathbf{q}) \in H^1$ for all $\mathbf{q} \in \tilde{Q}$ and moreover there exists uniform continuity in $H^1 \cap H^2$ with respect to data over $\tilde{Q}$ mainly $\|u(\mathbf{q})\|_{H^2} \leq K\|f\|_{L^2}$ where K is independent of $\mathbf{q} \in \tilde{Q}$, see Corollary 1.1, p. 222 [2] and Lemma 1.4, p. 223 [2] for a proof.

5.1 Continuity With Respect to Parameters

Let $\{\mathbf{q}^k\}$ be a sequence in $\tilde{Q}$ such that $\mathbf{q}^k \to \mathbf{q}$. We claim that $\mathbf{q} \in \tilde{Q}$ and $u(\mathbf{q}^k) \to u(\mathbf{q})$ weakly in H^2. The fact that $\mathbf{q} \in \tilde{Q}$ is obvious because we assume $\tilde{Q}$ is compact and there is at least a subsequence $\mathbf{q}^{k_j}$ that converges to $\mathbf{q}$ in $\tilde{Q}$. Furthermore $u(\mathbf{q})$ exists from the regularity of $u(\mathbf{q})$ over $\tilde{Q}$. Now let $u(\mathbf{q})$ satisfy the following weak formulation of the refractive index diffusion equation

$$\begin{aligned} \int_\Omega D\left(\nabla - 2\mathbf{n}_g\right) u(\mathbf{q}) \cdot \nabla v d\mathbf{x} \quad &+ \quad \int_\Omega \mu_a u(\mathbf{q}) v d\mathbf{x} + \frac{1}{2}\int_{\partial\Omega} u(\mathbf{q}) v ds \\ &= \quad -\int_\Omega \nabla F \cdot \nabla v d\mathbf{x} + \frac{1}{2}\int_{\partial\Omega} g^- v ds \end{aligned} \tag{39}$$

and let $u(\mathbf{q}^k)$ satisfy the following weak formulation:

$$\begin{aligned} \int_\Omega D^k\left(\nabla - 2\mathbf{n}_g^k\right) u(\mathbf{q}^k) \cdot \nabla v d\mathbf{x} \quad &+ \quad \int_\Omega \mu_a^k u(\mathbf{q}^k) v d\mathbf{x} + \frac{1}{2}\int_{\partial\Omega} u(\mathbf{q}^k) v ds \\ &= \quad -\int_\Omega \nabla F \cdot \nabla v d\mathbf{x} + \frac{1}{2}\int_{\partial\Omega} g^- v ds. \end{aligned} \tag{40}$$

Since we have uniform regularity of the solutions $u(\mathbf{q}^k)$ in $\tilde{Q}$, we have $u(\mathbf{q}^k)$ converges to some $w \in H^1(\Omega)$ which satisfies equation (39). Furthermore because of our parameters in $\mathbf{q}^k$ are bounded both above and below by zero, we can approximate these functions by continuous

functions and the fact that $u_{x_i}(\mathbf{q}^k)v$ is in $L^1(\Omega)$, we can take the limit in equation (40) and get (39). But the uniqueness of the solution to the refractive index diffusion approximation (see section 4), we deduce that $u = w$ in $H^1(\Omega)$. Therefore we have shown that $u(\mathbf{q}^k) \to u(\mathbf{q})$. This also guarantees that there exists a minimum of $J(\mathbf{q})$ in equation (27) because the compactness of the parameter space $\tilde{Q}$ combined with continuity of the solutions $u(\mathbf{q})$ with respect to the parameters $\mathbf{q} \in \tilde{Q}$ as well as the fact that $H^2(\Omega)$ is embedded in the space of continuous functions $C(\Omega)$ and the fact that point evaluation of $u(\mathbf{q})$ is a continuous operator.

6 Fréchet derivative

To minimize the cost functional $J(\mathbf{q})$ in equation (27), we need to derive the linearization of $T[q]$ (see section 3). Let us assume that nominal parameters D_0, $\mathbf{n}_{g0}$ and μ_0 exist for D, $\mathbf{n}_g$ and μ_a such that $D = D_0 + \alpha$, $\mathbf{n}_g = \mathbf{n}_{g0} + \beta$, and $\mu_a = \mu_0 + \gamma$ with α, β, and γ small. For simplicity, let us also assume $D = D_0$ and $\mathbf{n}_g = \mathbf{n}_{g0}$ near $\partial\Omega$. Let u_0 be the solution of,

$$\begin{aligned} \mu_a u_0(\mathbf{x}) - \nabla \cdot \left[D(\mathbf{x})\left(\nabla - 2\mathbf{n}_{g0}\right) u_0(\mathbf{x})\right] &= f_0(\mathbf{x}) \quad \text{in} \quad \Omega \\ u_0(\mathbf{x}) + 2D(\mathbf{x})\left(\frac{\partial}{\partial \nu} - 2\mathbf{n}_g \cdot \nu\right) u_0(\mathbf{x}) &= g^-(\mathbf{x}) \quad \text{on} \quad \partial\Omega. \end{aligned} \tag{41}$$

Let $u = u_0 + v$ where u solves equation (28) and subtracting equation (41) from equation (28), we obtain ignoring second order terms in α, β, γ, and v,

$$-\nabla \cdot D_0(x)\nabla v(x) + \mu_0(x)v(x) = \nabla \cdot \alpha(x)\nabla v_0(x) - \nabla \cdot 2D_0\beta(x)v_0(x) - \gamma v_0(x) \tag{42}$$

with boundary condition,

$$v(x) + 2D(x)\frac{\partial v}{\partial \nu}(x) = 0,\ x \in \partial\Omega. \tag{43}$$

The linearization $T'[q]$ is given by,

$$T'[q]\begin{pmatrix} \alpha \\ \beta \\ \gamma \end{pmatrix} = -D\frac{\partial v}{\partial \nu}, \tag{44}$$

where v is the solution to equation (42). The adjoint of this linearized equation (42) can be derived using the Green's formula

$$\int_\Omega \left(\left(\mu_a v - \nabla \cdot \left[D\left(\nabla - 2\mathbf{n}_g\right)v\right]\right)\bar{w}^* - v\overline{\left(\mu_a w^* - \nabla \cdot \left[D\left(\nabla - 2D\mathbf{n}_g\right)\right]w^*\right)}\right) d\Omega \tag{45}$$

$$= \int_{\partial\Omega} D\left(\frac{\partial v}{\partial \nu}\bar{w}^* - v\overline{\frac{\partial w^*}{\partial \nu}}\right) ds \tag{46}$$

and the adjoint of $T'[q]$is,

$$\left(T'[q]\begin{pmatrix} \alpha \\ \beta \\ \gamma \end{pmatrix}\right)^* r^* = \begin{pmatrix} -\nabla\bar{v}_0 \cdot \nabla w^* \\ 2D_0\bar{v}_0\nabla w^* \\ -\bar{v}_0 w^* \end{pmatrix} \tag{47}$$

where w^* is a solution of the adjoint equation

$$\mu_a(x)w^*(x) - \nabla \cdot [D(x)\left(\nabla - 2D(x)\mathbf{n}_g\right)w^*(x)] \;=\; 0 \tag{48}$$

with the boundary condition,

$$w^*(x) + 2D(x)\frac{\partial w^*}{\partial \nu}(x) \;=\; r^*,\; x \in \partial\Omega. \tag{49}$$

The linearization of $T[\mathbf{q}]$ for refractive index based diffusion optical tomography is inherently different than constant refractive index case. This is evident from the above equation where the nonconstant refractive index variation β results in a term of the form $2D_0\bar{v}_0\nabla w^*$ in the adjoint of $T'[\mathbf{q}]$. Therefore it is expected that the reconstruction of n may be substantially different than the reconstruction of D or μ_a.

7 SIMULATION RESULTS

We have performed some preliminary simulations using Matlab for both the forward and the inverse problem. In solving both problems we assumed the domain $\Omega \subset \mathbb{R}^2$ to be a circle of radius $43.0mm$ centered at the origin. We simulated a circular tumor of radius $10.0cm$ centered at $x = 15.0mm$, $y = 15.0mm$. The absorbtion coefficient (μ_a) was taken to be $0.012mm^{-1}$ inside the tumor and $0.006mm^{-1}$ outside the tumor. The diffusion coefficient (D) was taken to be $0.275mm$ inside the tumor and $0.55mm$ outside. The refractive index (n) was taken to be 1.2 inside the tumor and 1.0 outside. Figure 1a, b, and c illustrate these parameters as defined inside and outside the tumor. We begin by making a comparison of weak solutions for both the forward problem with constant refractive index and the forward problem with varying refractive index.

7.1 Forward problem simulation

For the absorbtion coefficient μ_a, diffusion coefficient D, and refractive index n, as shown in Figure 1, we simulated a tumor located in the upper right region of the domain using finite element method (FEM). The solutions are plotted in Figure 1 d and e. One should notice that while the solution to the forward problem with constant refractive index (Figure 1d) shows no indication of the simulated tumor, the solution to the forward problem with spatially varying refractive index (Figure 1e) shows a disturbance close to the location of the source. The semicircular band, where the intensity is noticeably less than the area around it, corresponds to where the gradient of the refractive index ∇n is large.

7.2 Inverse problem simulation

For each inverse problem simulation presented here we also show the meshes used to solve each of the forward problem and the inverse problem. The synthetic data used to conduct the simulations was generated by simulating a tumor by setting the parameters as in Figure 1a,b, and c and then interpolating these parameters onto the mesh used for the parameter estimation in the inverse problem (the exception is the simulation in Figure 7 which uses

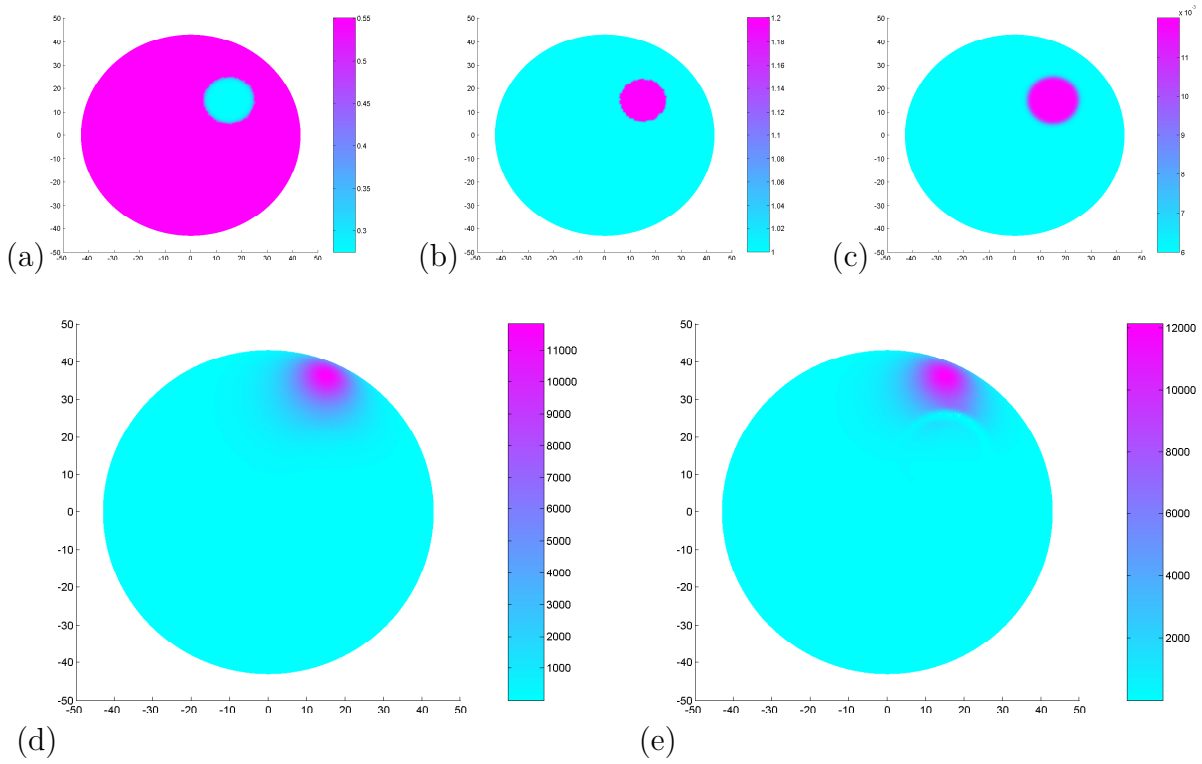

Figure 1: (a) The diffusion coefficient (D), (b) the refractive index (n), and (c) the absorbtion coefficient (μ_a), (d) forward problem solution for dc diffusion approximations with constant refractive index with varying D and μ_a as in (a) and (c), and (e) the forward problem solution for the dc diffusion approximation with spatially varying refractive index n as in (b) as well as spatially varying D and μ_a as in (a) and (c).

the forward problem mesh). The interpolated parameters are then used to solve the forward problem for each source and the data is taken to be the solution at the location of each detector for each source.

In solving the inverse problems, we used a finite difference method to estimate the Jacobian of the cost functional J. When noted, a simple iteratively regulated Gauss-Newton method was employed [16]. In these cases, the regularization parameter used for the kth iteration was $\lambda_k = \lambda/k$.

Figure 3a shows the refractive index used, along with analogously defined absorbtion (μ_a) and diffusion (D) coefficients, to generate the synthetic data from which the refractive index was then estimated (Figure 3 b) assuming a priori knowledge of both μ_a and D. The estimate was obtained by employing an iteratively regulated Gauss-Newton algorithm for 15 iterations. Overlaying each figure is the mesh used to define the basis functions for the parameters. The mesh used to solve the associated forward problem is shown in Figure 2. A comparison of the two shows little difference except perhaps a slight reduction in contrast upon examining the color scales for each figure.

Figure 4 shows the refractive index (Figure 4a) used, along with analogously defined μ_a and D coefficients, to generate the synthetic data from which the refractive index was then estimated (Figure 4b) assuming a priori knowledge of both μ_a and D. The estimate was

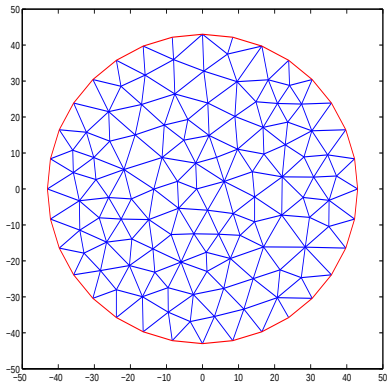

Figure 2: Mesh used to solve the forward problem associated with the inverse problem estimate in figures (3) and (6).

obtained by employing an iteratively regulated Gauss-Newton algorithm for 10 iterations. Overlaying each figure is the mesh used to define the basis functions for the parameters. The mesh used to solve the associated forward problem is shown in Figure 5. In this case, examining the color scales reveals some exaggeration in the contrast of the estimate.

Figure 6a shows the refractive index used, along with analogously defined μ_a and D, to generate the synthetic data from which the refractive index was then estimated (6b) while taking $\mu_a \equiv 0.006$ and $D \equiv 0.55$, the nominal values for these parameters. That is, we have neither assumed a priori knowledge of these parameters, nor have we tried to estimate them as we have done for the refractive index. The estimate was obtained by employing an iteratively regulated Gauss-Newton algorithm for 15 iterations. Overlaying each figure is the mesh used to define the basis functions for the parameters. Again the two figures show little difference save for some in contrast.

Figure 7a shows the refractive index used, along with analogously defined μ_a and D, to generate the synthetic data from which the refractive index was then estimated (Figure 7b) assuming a priori knowledge of both μ_a and D. The estimate was obtained by employing the Gauss-Newton algorithm for 30 iterations. Overlaying each figure is the mesh used to define the basis functions for the parameters. In this case a finer mesh was employed to define the parameters used to construct the synthetic data making the simulation more realistic. In addition, the mesh on the left is the same as that used to solve the forward problem. Again, here the contrast is exaggerated in the estimate and the image resolution is a bit lacking, as one would expect.

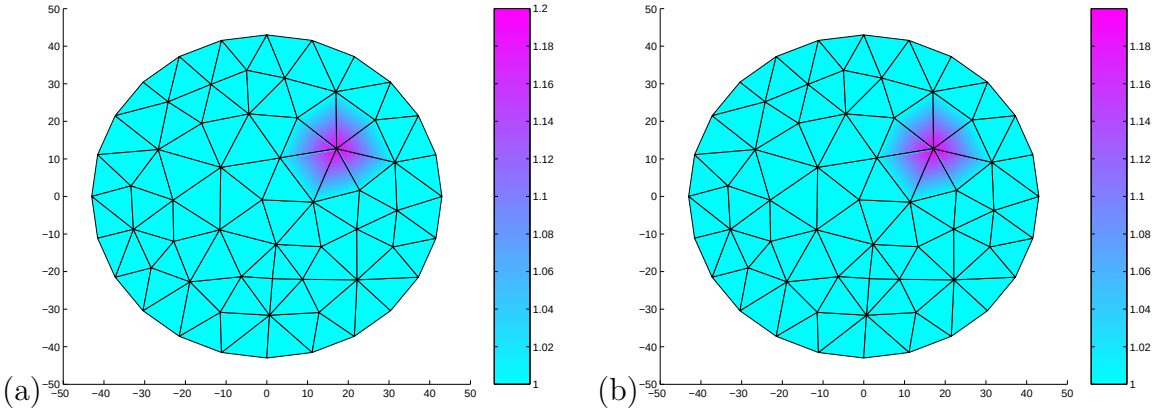

Figure 3: (a) The refractive index n used, with analogously defined μ_a and D, to generate the synthetic data from which the refractive index was then estimated assuming a priori knowledge of both μ_a and D. (b) the refractive index estimate which was obtained by employing an iteratively regulated Gauss-Newton algorithm for 15 iterations. Overlaying each figure is the mesh used to define the basis functions for the parameters. The mesh used to solve the associated forward problem is shown in Figure 2.

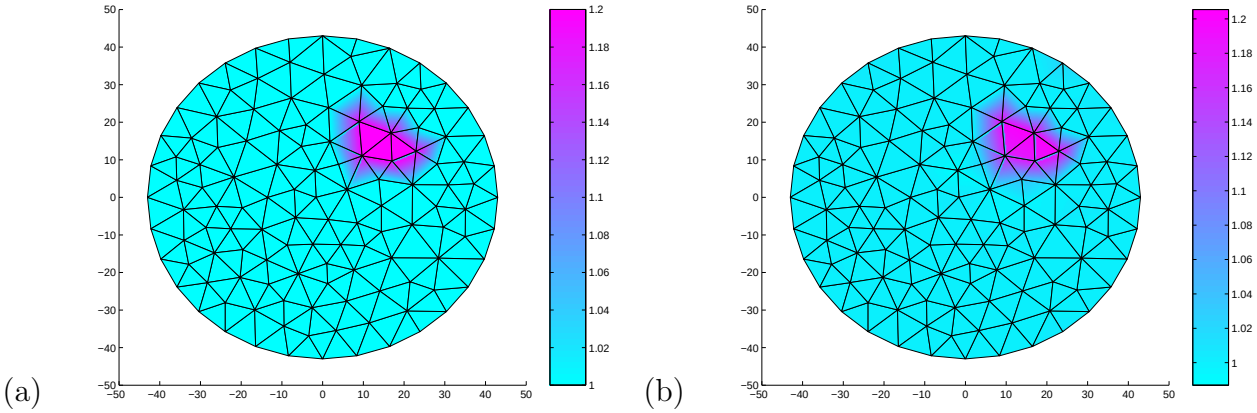

Figure 4: (a) The refractive index used, along with analogously defined μ_a and D, to generate the synthetic data from which the refractive index was then estimated (b) assuming a priori knowledge of both μ_a and D. (b) The refractive index estimate was obtained by employing an iteratively regulated Gauss-Newton algorithm for 10 iterations. Overlaying each figure is the mesh used to define the basis functions for the parameters. The mesh used to solve the associated forward problem is shown in Figure 5.

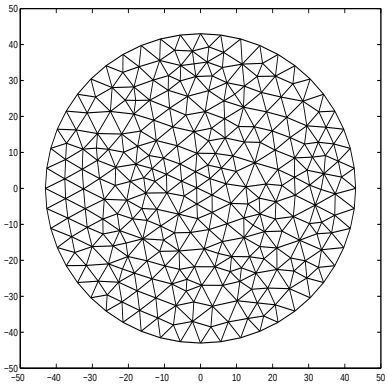

Figure 5: Mesh used to solve the forward problem associated with the inverse problem estimate in figures (4).

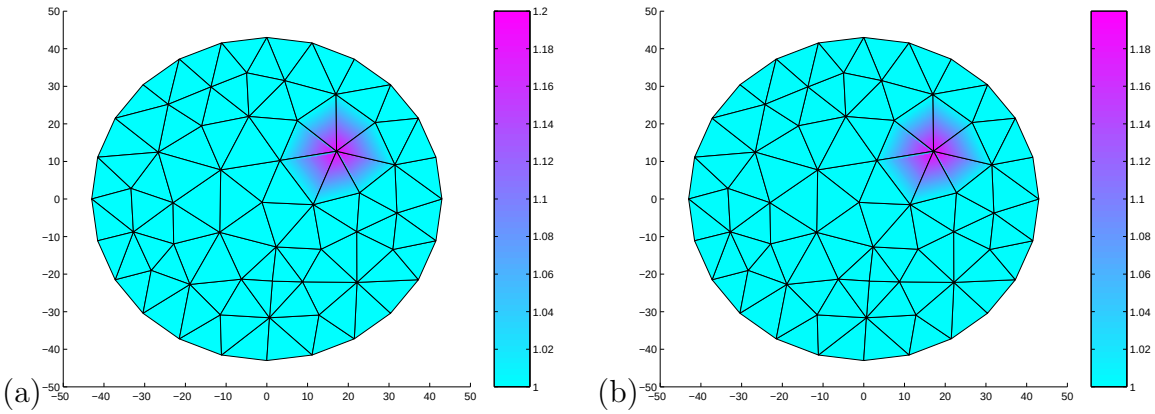

Figure 6: (a) The refractive index used, along with analogously defined μ_a and D, to generate the synthetic data from which the refractive index was then estimated (b) while taking $\mu_a \equiv 0.006$ and $D \equiv 0.55$, the nominal values for these parameters. (b) The refractive index estimate was obtained by employing an iteratively regulated Gauss-Newton algorithm for 15 iterations. Overlaying each figure is the mesh used to define the basis functions for the parameters.

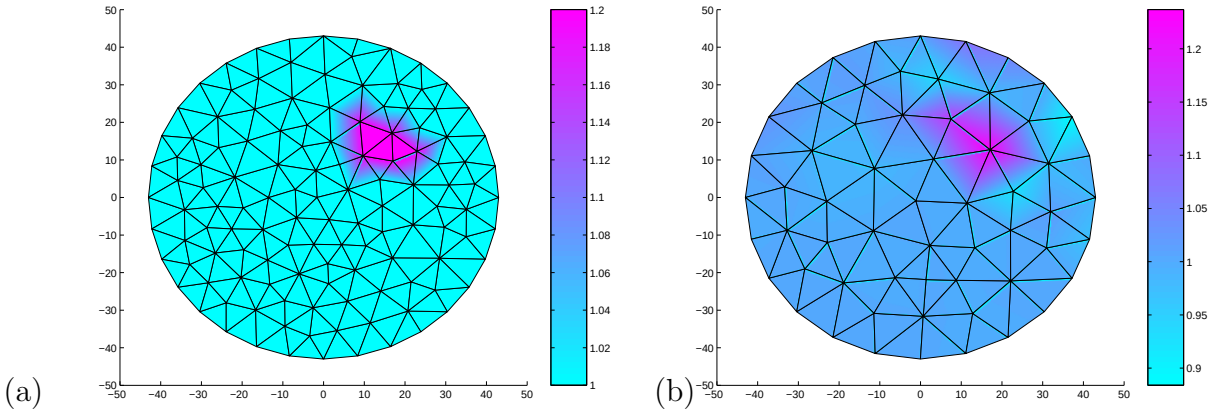

Figure 7: (a) The refractive index used, along with analogously defined μ_a and D, to generate the synthetic data from which the refractive index was then estimated (b) assuming a priori knowledge of both μ_a and D. (b) The refractive index estimate was obtained by employing the Gauss-Newton algorithm for 30 iterations. Overlaying each figure is the mesh used to define the basis functions for the parameters. In this case a finer mesh was employed to define the parameters used to construct the synthetic data. In addition, the mesh on the left is the same as that used to solve the forward problem.

8 CONCLUSIONS

In summary, we have derived a diffusion approximation to the radiative transport equation for a medium with a spatially varying refractive index. We established the well-posedness of the forward and the inverse problem for the new diffusion approximation. We also derive the Fréchet derivative of the nonlinear parameter to output map. Our simulations indicate that the refractive index based optical tomography shows promise for the reconstruction of the refractive index parameter. This is due to the inherent higher sensitivity of the refractive index parameter in the Jacobian of linearization of the inverse problem in comparison to the absorption and diffusion coefficients. We are currently investigating theoretical explanation for the higher sensitivity of the refractive index parameter.

References

[1] S.R. Arridge. Optical tomography in medical imaging: Topical review. *Inverse Problems*, 15:R41–R93, 1999.

[2] H.T. Banks and K. Kunisch. *Estimation Techniques for Distributed Parameter Systems.* Birkhauser, 2001.

[3] B. Chance and R.R. Alfano, editors. *Photon migration and imaging in random media and tissues*, volume 1888. SPIE, 1993.

[4] B. Chance and R.R. Alfano, editors. *Optical tomography, photon migration, and spectroscopy of tissue and model media: theory, human studies, and instrumentations, part 1 and 2*, volume 2389. SPIE, 1995.

[5] B. Chance, C.E. Cooper, D.T. Delpy, and E.O.R. Reynolds. Near-infrared spectroscopy and imaging of living systems. *Phil. Trans. R. Soc. Lond. B*, 352:643–648, 1997.

[6] National Research Council. *Mathematics and Physics of Emerging Biomedical Imaging.* National Academy Press, Washington DC, 1996.

[7] D. Daners. Robin boundary value problems on arbitrary domains. *Transactions of the American Mathematical Society*, 352(9):4207–4236, 2000.

[8] D.T. Delphy and M. Cope. Quantification in tissue near-infrared spectroscopy. *Phil. Trans. R. Soc. Lond. B*, 352:649–659, 1997.

[9] Z. Ding. A proof of the trace theorem of sobolev spaces on lipschitz domains. *Proceedings of the American Mathematical Society*, 124(2):591–600, 1996.

[10] G. B. Folland. *Introduction to Partial Differential Equations 2nd edition.* Princeton University Press, Princeton, NJ, 1995.

[11] J. Hebden, S.R. Arridge, and D.T. Delphy. Optical imaging in medicine: 1. experimental techniques. *Phys. Med. Biol.*, 42:825–840, 1997.

[12] A. Hielscher, R. Alcouffe, and R. Barbour. Comparison of finite-difference transport and diffusion calculations for photon migration in homogenous and heterogenous tissues. *Phys. Med. Biol.*, 42:1285–1302, 1998.

[13] H. Jiang. The diffusion approximation for turbid media with a spatially varying refractive index. *Proceedings of Advances in Optical Imaging and Photon Migration, Optical Society of America*, pages 366–368, 2000.

[14] T. Khan. On derivation of the radiative transfer equation and its diffusion approximation for scattering media with spatially varying refractive indices. *Clemson University Mathematical Sciences Technical Report*, TR2003-07-TK:1–6, July 2003.

[15] T. Khan and H. Jiang. A new diffusion approximation to the radiative transfer equation for scattering media with spatially varying refractive indices. *J. Opt. A: Pure Appl. Opt.*, 5:137–141, 2003.

[16] T. Khan and A. Smirnova. 1d inverse problem in diffusion based optical tomography using iteratively regularized gauss-newton algorithm. *Applied Mathematics and Computation*, 161:149–170, 2005.

[17] T. Khan and A. Thomas. Comparison of p_n or spherical harmonics approximation for scattering media with spatially varying and spatially constant refractive indices. *Optics Communications*, in press, 2005.

[18] T. Khan and A. Thomas. On derivation of the radiative transfer equation and its spherical harmonics approximation for scattering media with spatially varying refractive indices. *Clemson University Mathematical Sciences Technical Report*, TR2004-12-KT:1–49, December 2004.

[19] M. Klibanov and T.R. Lucas. Numerical solution of a parabolic inverse problem in optical tomography using experimental data. *SIAM J. Appl. Math.*, 59(5):1763–1789, 1999.

[20] L. Marti-Lopez, J. Bouza-Dominguez, and J. Hebden. Interpretation of the failure of the time-dependent diffusion equation near a point source. *Optics Communications*, In Press, 2004.

[21] L. Marti-Lopez, J. Bouza-Dominguez, J. Hebden, S. Arridge, and R. Martinez-Celorio. Validity conditions for the radiative transfer equation. *J. Opt. Soc. Am. A*, 20(11):2046–2056, 2003.

[22] V. G. Mazĺja. *Sobolev Spaces*. Springer, Berlin, 1985.

[23] MC Roggermann, BM Welsh, PJ Gardner, RL Johnson, and BL Pedersen. Sensing three-dimensional index-of-refraction variations by means of optical wavefront sensor measurements and tomographic reconstruction. *Optical Engineering*, 34(5):1374–1384, 1995.

[24] GJ Tearney, ME Brezinski, JF Southern, BE Bouma, MR Hee, and JG Fujimoto. Determination of the refractive index of highly scattering human tissue by optical coherence tomography. *Optics Letters*, 20(21):2258–2260, 1995.